Adv. Polar Upper Atmos. Res., **17**, 1–12, 2003

Effects of the stratospheric sudden warming on the temperature in the MLT region

Yasunobu Miyoshi

Department of Earth and Planetary Sciences, Kyushu University, Hakozaki, Higashi-ku, Fukuoka 812-8581

(Received December 19, 2002; Accepted March 25, 2003)

Abstract: We investigate effects of the stratospheric sudden warming on the temperature in the MLT (mesosphere and lower thermosphere) region by using a general circulation model up to 150 km height. Cooling of 5–15 K at high latitudes of the upper mesosphere and lower thermosphere occurs during the stratospheric sudden warming event. The result indicates influences of the stratospheric sudden warming on the temperature in the MLT region. We investigate mechanisms of the temperature variation at high latitudes of the upper mesosphere and lower thermosphere associated with the stratospheric sudden warming event.

key words: planetary wave, stratospheric sudden warming, MLT region

1. Introduction

The stratospheric sudden warming during the mid-winter (SSW, hereafter) is well known, and is caused by vertical propagation of the amplified planetary wave from the troposphere (Matsuno, 1971). Features of the general circulation in the stratosphere during the SSW are reported by many studies (*e.g.* Dunkerton *et al*., 1981; Palmer, 1981).

Labitzke (1972) showed cooling in the mesosphere during the SSW, and Hirota and Bernett (1977; HB77 hereafter) showed cooling of 10 K at high latitudes of 80 km height during the SSW by using the Nimbus 6 satellite data. Recently, by using the lidar and airglow measurements, the temperature in the MLT (mesosphere and lower thermosphere) region has been obtained. Walterscheid *et al.* (2000) reported cooling of 25 K during the SSW in February 1993 over Eureka, Canada. These results indicate a connection between the temperature in the polar MLT region and the SSW.

By using a 2-dimensional mechanistic model, Holton (1983) studied effects of the SSW on the general circulation in the mesosphere. He shows that cooling in the polar mesosphere is accompanied by warming in the polar stratosphere. He suggests that cooling in the polar mesosphere is mainly caused by the radiative cooling. However, in his model, only a single zonal wavenumber is taken into account. The upper boundary of his model is about 90 km height, so that effects of the SSW on the temperature above the mesopause region can not be studied.

Because there is only a few temperature measurements at high latitudes of the MLT region, effects of the SSW on the temperature in the MLT region is not well understood. Mechanisms of the cooling in the mesopause region are not clear. Thus, the purpose of this study is to investigate effects of the SSW on the temperature in the MLT region by using a general circulation model (GCM) with upper boundary at 150 km height. Heat balance at high latitudes of the MLT region during the SSW is analyzed in detail. The descriptions of the GCM used in this study are presented in Section 2. Results are presented in Section 3. Discussions and summary follow in Section 4.

2. Model descriptions

In this study, a GCM developed at Kyushu University is used. The GCM is a global spectral model with the triangular truncation at wavenumber 21 in the horizontal direction. The GCM has 55 vertical levels and contains the region from the ground to about 150 km height. The detailed descriptions of the GCM are found in Miyoshi (1999) and Miyahara *et al.* (1993), so the description of the GCM is briefly mentioned here.

The GCM has a full set of physical processes, such as radiation, a boundary layer, hydrology, moist and dry convection and vertical eddy diffusion. In the troposphere, stratosphere and mesosphere, the radiation code developed at CCSR, University of Tokyo (Nakajima *et al*., 2000) is used. In the lower thermosphere, Fomichev's parameterization (1993) is used for the long wave radiation by CO_2. The long wave radiation by NO is also parameterized by Kockarts's method (Kockarts, 1980). Strobel's parameterization (Strobel, 1978) is used for the solar radiation by O_2. The distributions of O_3, CO_2 and NO are climatologically prescribed. In the upper mesosphere and lower thermosphere, the density of the atmosphere becomes extremely low, so that the diffusion of momentum and heat due to the molecular viscosity and conductivity is introduced. Furthermore, the momentum exchange between the neutral atmosphere and the ionized atmosphere is also taken into account, because the density of the ionized atmosphere is not negligible. Below 95 km height, effects of unresolved orographic and non-orographic gravity waves are included. The parameterization by McFarlane (1987) is used for orographic gravity waves, while the parameterization by Lindzen (1981) is used for non-orographic gravity waves. For Lindzen's parameterization, a simple wave spectrum consisting of zonal phase speeds 0, ± 10, ± 20 and ± 30 m/s is taken into account.

The numerical integration is performed over successive 4 years. The mid-winter SSW occurs in the second and fourth years. In this study, features of the general circulation during the SSW in the second year are analyzed.

3. Results

3.1. Temperature

Figure 1 shows time variation of the zonal mean temperature at 80°N of 30 km and 40 km. Latitude-height plots of the zonal mean zonal wind for 5 January (before the SSW) and 11 January (during the SSW) are shown in Fig. 2. The westerly with the

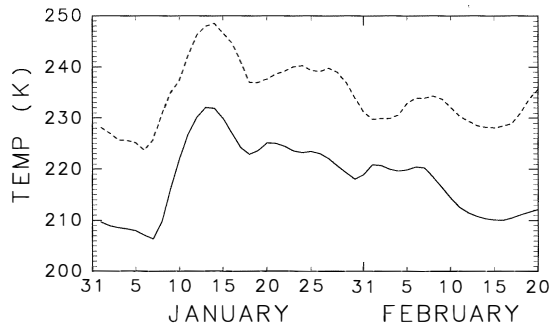

Fig. 1. Time series of the zonal mean temperature at 80°N of 30 km (solid line) and 40 km (dotted line). Units are K.

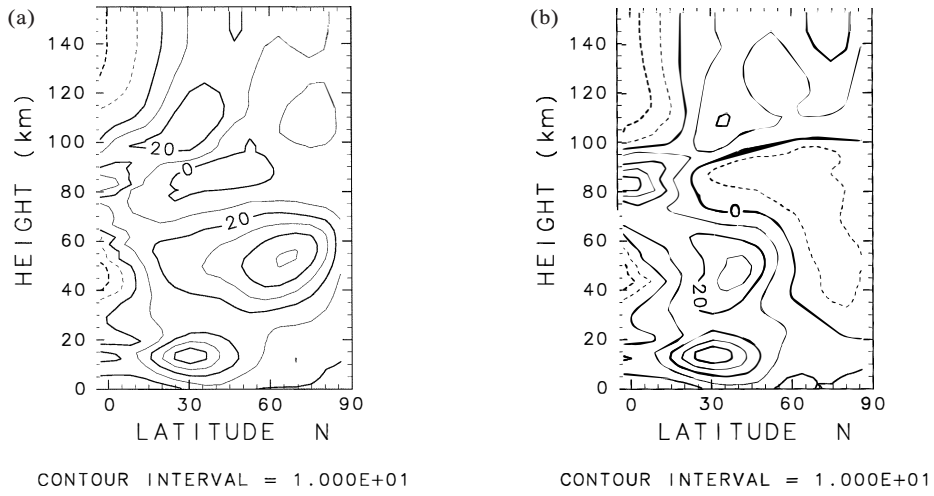

Fig. 2. (a) Latitude-height plot of the zonal mean zonal wind on 5 January. Contour interval is 10 m/s. Solid and dotted lines represent westerly and easterly, respectively.
(b) As in Fig. 2a bur for on 11 January.

maximum speed of 50 m/s prevails in the stratosphere and mesosphere before the SSW. During the SSW, the broad region of the easterly appears in high latitudes of the stratosphere and mesosphere. Figures 3a and 3b show the zonal mean temperature for 5 January and 11 January. It is clearly seen that the temperature at high latitudes of the stratosphere rises during the period from 5 January to 11 January. Thus, a major sudden warming occurs around 10 January. These features are similar to the observed features. Weak warmings also occur at 40 km height around 25 January and 5 February.

Effects of the SSW on the temperature at high latitudes of the mesopause region are examined. Figure 4a shows time variation of the zonal mean temperature at 80°N of 80 km and 90 km. At 80 km height, cooling of 10 K occurs around 10 January, and the

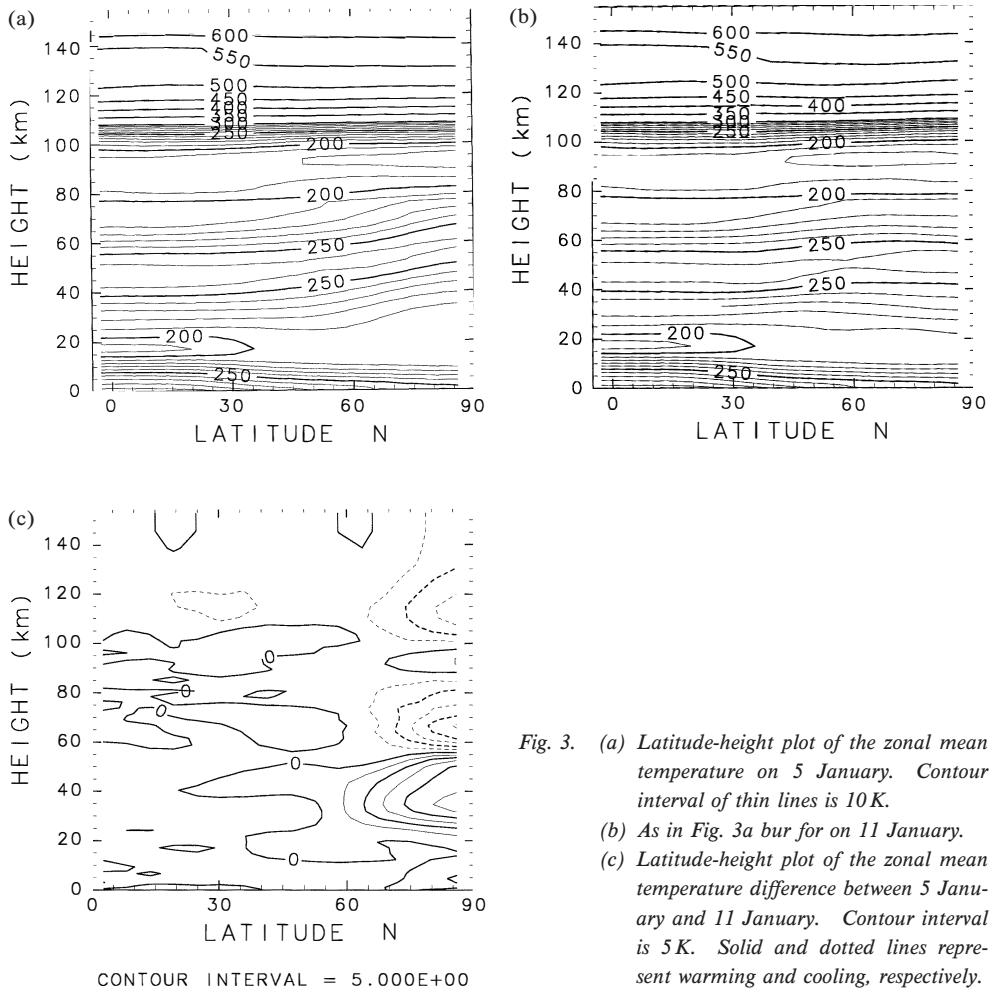

Fig. 3. *(a) Latitude-height plot of the zonal mean temperature on 5 January. Contour interval of thin lines is 10 K.*
(b) As in Fig. 3a bur for on 11 January.
(c) Latitude-height plot of the zonal mean temperature difference between 5 January and 11 January. Contour interval is 5 K. Solid and dotted lines represent warming and cooling, respectively.

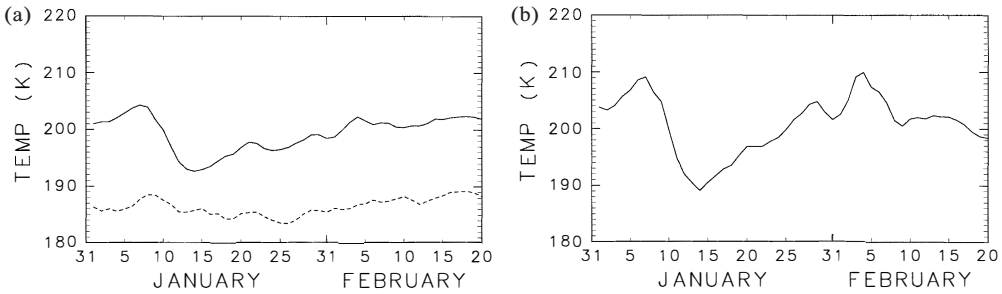

Fig. 4. *(a) Time series of the zonal mean temperature at 80°N of 80 km (solid line) and 90 km (dotted line). Units are K.*
(b) Time series of the temperature at 85°W, 80°N of 80 km. Unit is K.

cooling rate is 2.5 K/day. Weak coolings occur around 25 January and 5 February. It is clearly seen that time variation of the temperature at 80 km is negatively correlated with the temperature variation at 30 km. The cooling during 10 January does not occur at 90 km. The reason why cooling does not occur at 90 km will be discussed at Section 3.3.

Here, the global distribution of the temperature difference between the pre-SSW period and the SSW period is examined. Figure 3c shows the zonal mean temperature difference between 5 January and 11 January. Warming at high latitudes of the stratosphere is accompanied by cooling at high latitudes of the mesosphere. The cooling region extends up to 90 km height. The cooling in the lower mesosphere is consistent with Labitzke (1972). Cooling of 10 K at high latitudes of 80 km height during the SSW event is consistent with HB77 obtained by the Nimbus 6 satellite data.

Waltersheid *et al.* (2000) performed numerical simulation for the SSW in February 1993 by using the TIME-GCM. They also showed cooling of 10 K in the polar mesopause region during the SSW. Furthermore, in their paper, the lidar and airglow measurement recorded cooling of 25 K at the mesopause over Eureka, Canada (85°W, 80°N) during the SSW event in February 1993, which is larger than the results obtained by HB77 and this study. Figure 4b shows time variation of the simulated temperature at 85°W, 80°N of 80 km height (over Eureka). The temperature over Eureka simulated by the GCM shows cooling of 20 K during the SSW, and this cooling is comparable to the observed cooling over Eureka. This result suggests that cooling of the zonal mean temperature in February 1993 is smaller than 25 K cooling.

Above 100 km height, cooling occurs at all latitudes of the northern hemisphere. At high latitudes of 105–130 km, cooling of 10–15 K is seen. Figures 5a and 5b show

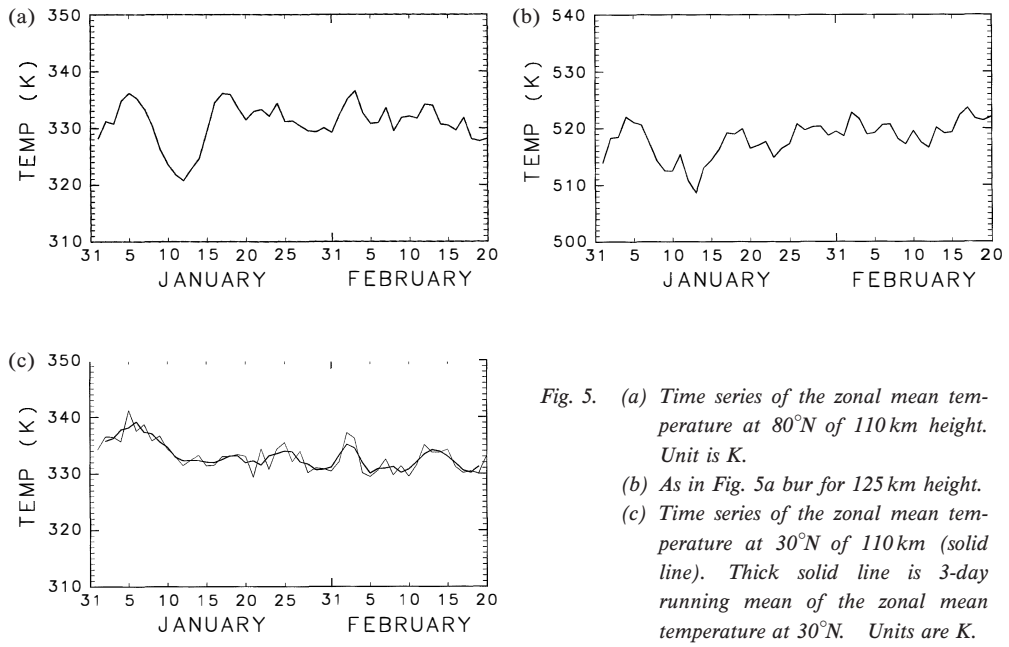

Fig. 5. *(a) Time series of the zonal mean temperature at 80°N of 110 km height. Unit is K.*
(b) As in Fig. 5a bur for 125 km height.
(c) Time series of the zonal mean temperature at 30°N of 110 km (solid line). Thick solid line is 3-day running mean of the zonal mean temperature at 30°N. Units are K.

time variation of the zonal mean temperature at 80°N of 110 km and 125 km, respectively. In the lower thermosphere, the temperature variation with time scales of a few days is dominant. Cooling more than 10 K around 10 January is significant, and is accompanied by the SSW event. Thus, this result indicates that the temperature at high latitudes of the lower thermosphere is influenced by the temperature variation in the stratosphere.

Next, we investigate time variation of the zonal mean temperature at middle latitudes of 110 km height (Fig. 5c). Cooling of 7 K appears around 10 January, and weak coolings occur around 27 January and 5 February. These coolings are accompanied by coolings at high latitudes. Thus, these results indicate a correlation between the temperature at 110 km height and the stratospheric temperature.

3.2. Heat balance

We consider the temperature change on the basis of the quasi-geostrophic transformed Eulerian mean (TEM) thermodynamic equation in log-pressure coordinates using standard notations (Andrews *et al*., 1987):

$$\frac{\partial \overline{T}}{\partial t} \cong -\frac{H}{R} N^2 \overline{w}^* + \frac{\overline{J}}{C_p}.$$

The first term and the second term of the right hand side denote the contribution of vertical motion and diabatic heating, respectively. In the middle atmosphere, the diabatic heating is almost equal to the radiative heating. Figure 6 shows the contribution of vertical motion and radiative heating at 80°N of 80 km height. Before the SSW, the temperature rises, because heating due to the downward motion exceeds cooling due to the radiation. On the other hand, during the SSW, the contribution of vertical motion is small. The weak upward motion takes place on 10 January to 12 January, and cooling due to the vertical motion appears. The cooling during the SSW is mainly due to the radiative cooling. After the SSW event, the enhancement of heating due to the downward motion occurs, and the temperature rises again.

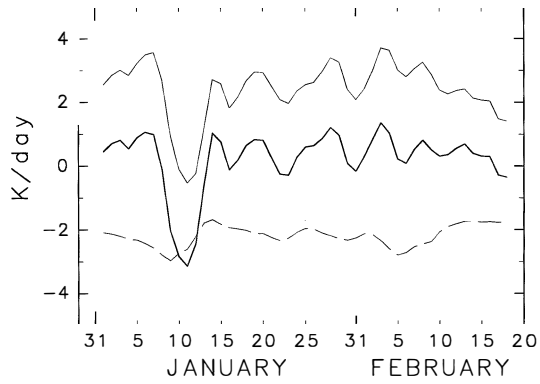

Fig. 6. Time series of heat balance at 80°N of 80 km. Thin solid line and dotted line represent the contribution of vertical motion and the contribution of radiation, respectively. Thick solid line represents the contribution of vertical motion plus the radiation. Units are K/day.

Figure 7 shows the contribution of vertical motion and radiative heating at 80°N of 110 km height. Features of heat balance at 110 km are similar to those at 80 km. During the SSW, heating due to the downward motion becomes weak. The temperature falls because cooling due to the radiation exceeds heating due to the downward motion. Thus, time variation of the temperature is closely related with the strength of the vertical motion.

Figure 8 shows the residual mean meridional circulation before the SSW and during the SSW. During the SSW, the strong downward motion at high latitudes of the stratosphere is accompanied by the very weak vertical motion in the polar mesosphere. The weak upward motion appears at 80°N of the upper mesosphere. At high latitudes

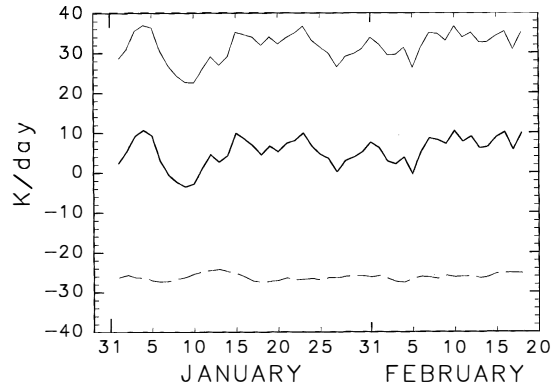

Fig. 7. As in Fig. 6 but for 110 km.

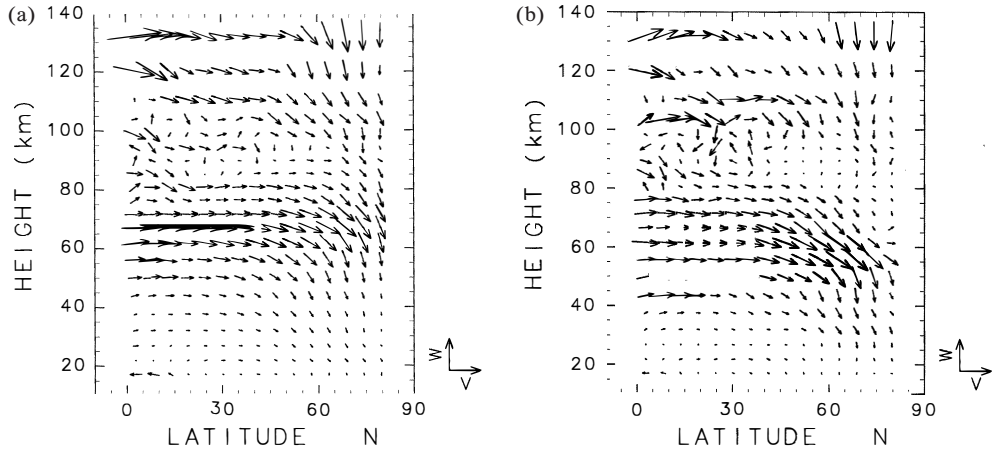

Fig. 8. (a) The residual mean meridional circulation averaged over 4 January through 6 January. The unit vectors shown at the right side bottom represent the poleward wind of 10 m/s and the upward motion of 5 cm/s.

(b) As in Fig. 8a but for averaged over 9 January through 11 January.

above 100 km height, the downward motion during the SSW is weaker than that before the SSW.

3.3. *Wave drag*

We consider time variation of the vertical motion on the basis of the TEM equation. It is well known that the wave drag (the E-P flux divergence) is responsible for maintaining the residual circulation (Andrews *et al*., 1987):

$$-f\bar{v}^* \cong \overline{G},$$

$\overline{G}$ is the wave drag, which in the middle atmosphere is mainly due to the planetary wave and the gravity wave. In the winter hemisphere, the poleward wind is driven by easterly acceleration by the wave drag. The GCM used in this study is a T21 model, so that the wave drag due to the zonal wavenumber up to 21 is resolved. The wave drag due to the smaller scale gravity wave is estimated by the gravity wave drag parameterizations (McFarlane, 1987; Lindzen, 1981). Figure 9a shows a latitude-height plot of the wave drag due to the resolved waves and the small-scale gravity waves before the SSW. As a result of the strong easterly acceleration due to the wave drag at 60 to 80 km height, the poleward wind at middle latitudes and the downward motion at high latitudes are strong at 60 to 80 km height. Above 100 km height, easterly acceleration due to the wave drag appears, and this easterly acceleration also induces the poleward and downward winds. At 90 to 100 km height, the wave drag is weak, and this is a reason why the meridional and vertical winds are weak. Because the downward motion at the polar region of 90 km remains quite small during the whole period, time variation of the temperature at 90 km is small during the SSW.

Figure 9b shows a latitude-height plot of the wave drag during the SSW (averaged over 9 January through 11 January). Figure 9c shows the difference of the wave drag between the pre-SSW period and the SSW period. The enhancement of easterly acceleration at high latitudes of the stratosphere and lower mesosphere is accompanied by the reduction of easterly acceleration at high latitudes above 65 km height. Thus, during the SSW, the reduction of easterly acceleration makes the downward motion above 65 km weaker.

Next, effects of the gravity wave drag on the meridional circulation are examined. Figure 10a is the difference of the wave drag due to the gravity wave drag parameterization between the pre-SSW period and the SSW period, while Fig. 10b is the difference due to the planetary wave (the zonal wavenumber 1 to 3). The difference of the wave drag due to waves whose zonal wavenumber is 4 to 21 is negligibly small. At 50 to 95 km height, easterly acceleration due to the gravity wave drag during the SSW is weaker than that before the SSW. Before the SSW, the westerly jet prevails at high latitudes of the stratosphere and mesosphere, so that upward propagation of westward-moving gravity waves occurs easily. However, during the SSW, due to the easterly wind at high latitudes, upward propagation of westward-moving gravity waves is prohibited. Moreover, upward propagation of eastward-moving gravity waves is allowed. At high latitudes of the upper mesosphere, westerly acceleration due to the gravity wave drag is seen (not shown). At 65 to 90 km height, the reduction of easterly acceleration in Fig. 9c is caused by the reduction of easterly acceleration due to the gravity wave drag.

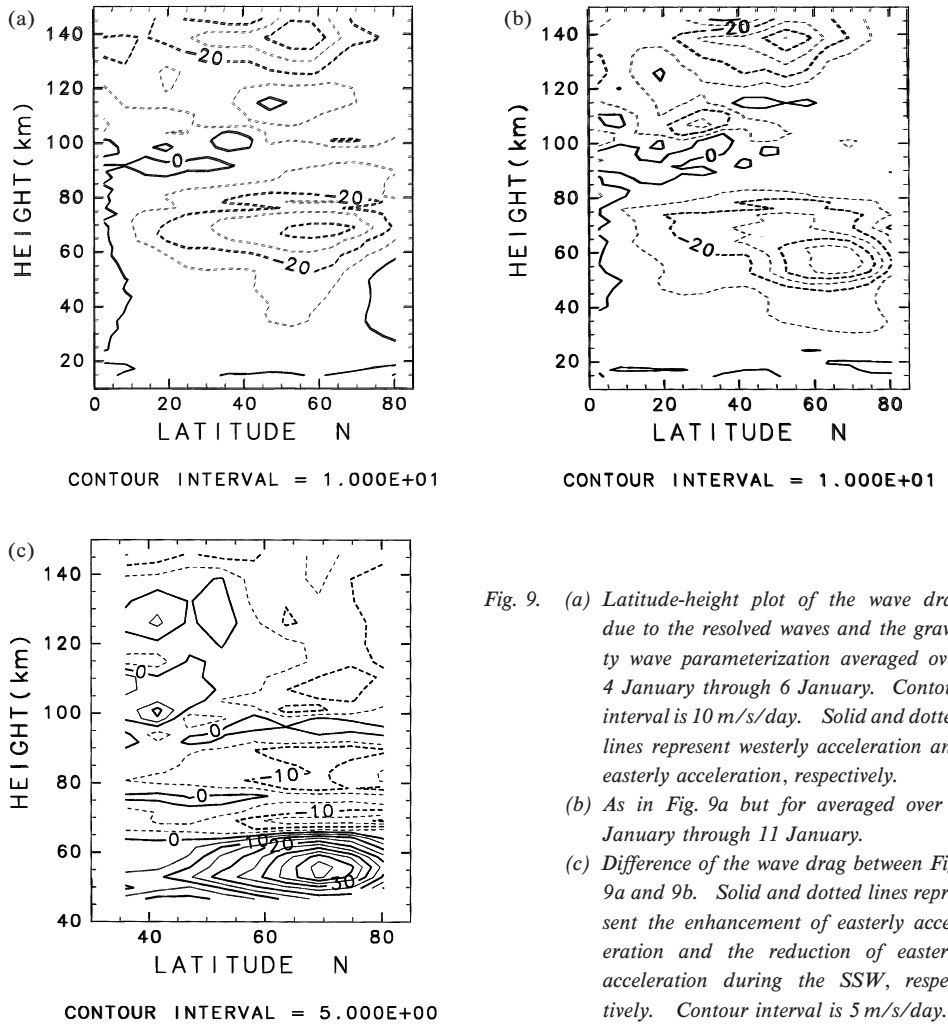

Fig. 9. *(a) Latitude-height plot of the wave drag due to the resolved waves and the gravity wave parameterization averaged over 4 January through 6 January. Contour interval is 10 m/s/day. Solid and dotted lines represent westerly acceleration and easterly acceleration, respectively.*
(b) As in Fig. 9a but for averaged over 9 January through 11 January.
(c) Difference of the wave drag between Fig. 9a and 9b. Solid and dotted lines represent the enhancement of easterly acceleration and the reduction of easterly acceleration during the SSW, respectively. Contour interval is 5 m/s/day.

Thus, the reduction of easterly acceleration due to the gravity wave drag weakens the meridional circulation at the poleward of 60°N at 65 to 90 km height.

Holton (1983) investigated the behavior of the gravity wave during the SSW by using a 2-dimensional mechanistic model. He showed that the meridional circulation in the mesosphere was affected by the reduced gravity wave drag during the SSW. His result is consistent with our result.

Above 105 km height of high latitudes, the wave drag due to the planetary wave during the SSW period is weaker than that during the pre-SSW period (Fig. 10b). Before the SSW, the quasi-stationary planetary wave with the zonal wavenumber 1 appears above 105 km height of high latitudes (Fig. 11a). This is due to upward propagation of the planetary wave from the stratosphere into the lower thermosphere, because the weak easterly wind exists only at 30 to 60°N near the mesopause. On the

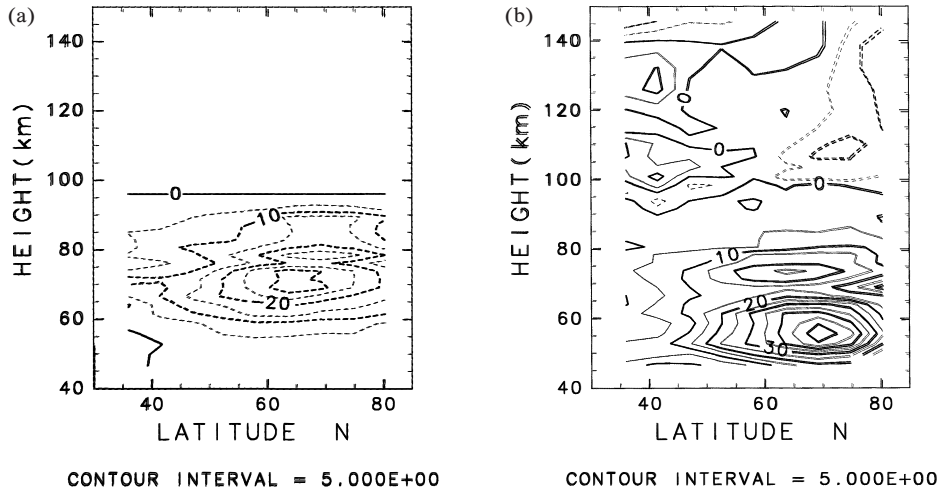

Fig. 10. *(a) As in Fig. 9c but for the difference of the wave drag due to the gravity wave drag. (b) As in Fig. 9c but for the difference of the wave drag due to the planetary wave (the zonal wavenumber 1–3).*

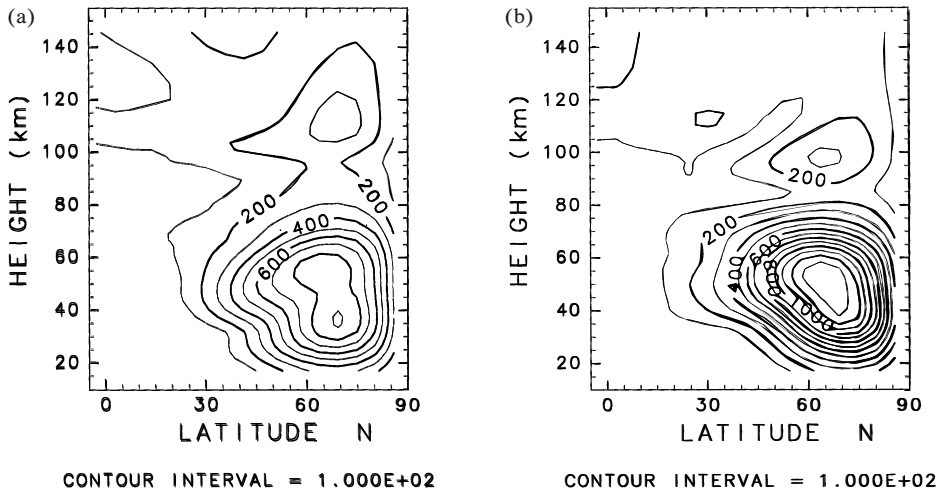

Fig. 11. *(a) Latitude-height plot of the amplitude of the zonal wavenumber 1 component averaged over 3 January through 7 January. Effects of tidal waves are excluded. Contour interval is 100 m. (b) As in Fig. 11a but for averaged over 9 January through 13 January.*

other hand, during the SSW, the amplitude of the planetary wave above 105 km is weak, because upward propagation of the planetary wave is inhibited by the easterly wind in the stratosphere and mesosphere. Thus, the reduction of easterly acceleration due to the planetary wave during the SSW weakens the poleward wind and downward motion above 105 km.

Above 105 km height, the difference of the planetary wave amplitude between the pre-SSW period and the SSW period is small as compared with that in the stratosphere. The difference of the magnitude of the downward motion between the pre-SSW period and the SSW period is also small above 105 km height. However, changes of heating rate during the SSW are large (Fig. 7). The buoyancy frequency in the lower thermosphere is very large, so that small changes of the magnitude of the downward motion produce large changes of heating rate during the SSW.

4. Discussions and summary

In this study, effects of the SSW on the general circulation in the upper mesosphere and lower thermosphere are investigated by using a GCM. The results are as follows.

- Cooling of ~10 K at high latitudes of the upper mesosphere occurs during the SSW, while cooling of 5–15 K occurs at high latitudes of the lower thermosphere.
- The cooling during the SSW is mainly caused by cooling due to the radiation.
- The reduction of easterly acceleration due to the gravity wave drag during the SSW weakens the downward motion at high latitudes of the upper mesosphere. In the lower thermosphere, the reduction of easterly acceleration due to the planetary wave during the SSW makes the downward motion at high latitudes weaker.
- Time variation of the temperature around 90 km height at high latitudes is small during the SSW. This is due to weak wave drag around 90 km height.

These results show that the temperature in the MLT region is influenced by the SSW. Labitzke (1987) investigated interannual variability of the SSW. She showed that more major stratospheric mid-winter warmings occurred in the easterly phase of the stratospheric Quasi-Biennial Oscillation (QBO, hereafter), and the relatively few major mid-winter warmings observed in the westerly phase of the QBO took place only when the sunspot number was high. These results suggest that the QBO influences the cooling in the polar MLT region associated with the SSW. There may be a correlation between the QBO and interannual variability of the temperature in the polar MLT region. However, only a few observations about the temperature in the polar MLT region have been reported. Interannual variability of the temperature in the MLT region is not well understood. Model studies for interannual variability in the MLT region will be required.

The results in this study show that the SSW event influences the temperature above 130 km height. The upper boundary of our GCM is 150 km height, so that effects of the SSW on the temperature variation above 150 km can not be simulated. Numerical simulation by a thermosphere general circulation model is necessary to investigate thermospheric responses of the SSW.

Acknowledgments

I wish to thank Profs. T. Hirooka and S. Miyahara for their helpful discussions and comments. I also thank Prof. I. Hirota of Kyoto University for kindly advices. I am grateful to the referees for their helpful comments on my original manuscript. The GFD-DENNOU Library was used for drawing the figures. This research was

financially supported by a Grant-in-Aid for Scientific Research by the Ministry of Education, Science, Sports and Culture, Japan.

The editor thanks the referees for their help in evaluating this paper.

References

Andrews, D.G., Holton, J.R. and Leovy, C.B. (1987): Middle Atmosphere Dynamics. San Diego, Academic Press, 489 p.

Dunkerton, T., Hsu, C.-P.F. and McIntyre, M.E. (1981): Some eulerian and lagrangian diagnostics for a model stratospheric warming. J. Atmos. Sci., **38**, 819–843.

Fomichev, V.I., Kutepov, A.A., Akmaev, R.A. and Shved, G.M. (1993): Parameterization of the 15 μm CO_2 band cooling in the middle atmosphere (15–115 km). J. Atmos. Terr. Phys., **55**, 7–18.

Hirota, I. and Barnett, J.J. (1977): Planetary waves in the winter mesosphere-preliminary analysis of Nimbus 6 PMR results. Q.J.R. Meteorol. Soc., **103**, 487–498.

Holton, J.R. (1983): The influence of gravity wave breaking on the general circulation of the middle atmosphere. J. Atmos. Sci., **40**, 2497–2507.

Kockarts, G. (1980): Nitric oxide cooling in the terrestrial thermosphere. Geophys. Res. Lett., **7**, 137–140.

Labitzke, K. (1972): Temperature changes in the mesosphere and stratosphere connected with circulation changes in winter. J. Atmos. Sci., **29**, 756–766.

Labitzke, K. (1987): Sunspots, the QBO and the stratospheric temperature in the north polar region. Geophys. Res. Lett., **14**, 535–537.

Lindzen, R.S. (1981): Turbulence and stress owing to gravity wave and tidal breakdown. J. Geophys. Res., **86**, 9707–9714.

McFarlane, N.A. (1987): The effect of orographically excited gravity wave drag on the general circulation of the lower stratosphere and troposphere. J. Atmos. Sci., **44**, 1775–1800.

Matsuno, T. (1971): A dynamical model of the stratospheric sudden warming. J. Atmos. Sci., **28**, 1479–1494.

Miyahara, S., Yoshida, Y. and Miyoshi, Y. (1993): Dynamic coupling between the lower and upper atmosphere by tides and gravity waves. J. Atmos. Terr. Phys., **55**, 1039–1053.

Miyoshi, Y. (1999): Numerical simulation of the 5-day and 16-day waves in the mesopause region. Earth, Planets Space, **51**, 763–772.

Nakajima, T., Tsukamoto, M., Tsushima, Y., Numaguchi, A. and Kimura, T. (2000): Modeling of the radiative process in an atmospheric general circulation model. Appl. Opt., **39**, 4869–4878.

Palmer, T.N. (1981): Diagnostic study of a wavenumber-2 stratospheric sudden warming in a transformed Eulerian-mean formalism. J. Atmos. Sci., **38**, 844–855.

Strobel, D.F. (1978): Parameterization of the atmospheric heating rate from 15 to 120 km due to O_2 and O_3 absorption of solar radiation. J. Geophys. Res., **83**, 6225–6230.

Walterscheid, R.L., Sivjee, G.G. and Roble, R.G. (2000): Mesospheric and lower thermospheric manifestations of a stratospheric warming event over Eureka, Canada (80°N). Geophys. Res. Lett., **27**, 2897–2900.